

High order discretization methods for spatial dependent SIR models

Bálint Takács*

Yiannis Hadjimichael†

March 23, 2022

Abstract

In this paper, an SIR model with spatial dependence is studied, and results regarding its stability and numerical approximation are presented. SIR models have been used to describe epidemic propagation phenomena, and one of the first models is derived by Kermack and McKendrick in 1927 [13]. In such models, the population is split into three classes: S being the group of healthy individuals, who are susceptible to infection; I is the compartment of the ill species, which can infect other individuals; and R being the class in which recovered species are.

We consider a generalization of the original Kermack and McKendrick model in which the size of the populations differs in space. The use of local spatial dependence yields a system of integro-differential equations. The uniqueness and qualitative properties of the continuous model are analyzed. Furthermore, different choices of spatial and temporal discretizations are deployed, and step-size restrictions for population conservation, positivity and monotonicity preservation of the discrete model are investigated. We provide sufficient conditions under which high order numerical schemes preserve the discrete properties of the model. Computational experiments verify the convergence and accuracy of the numerical methods.

1 Introduction

During the millenia of the history of mankind, several epidemics have raved the population. Since the plague of Athens in 430 BC described by historian Thucydides (one of the earliest description of such epidemics), researchers tried to model and describe the outbreak of illnesses. Nowadays most of the models used in science are derived from the original ideas of Kermack and McKendrick [13], who constructed a compartment model to study the process of epidemic propagation. In their model the population is split into three classes: S being the group of healthy individuals, who possibly will be infected; I is the compartment of the ill people, who can infect other individuals; and R being the class of recovered or immune individuals.

*Applied Analysis and Computational Mathematics, MTA-ELTE Numerical Analysis and Large Networks Research Group, Eötvös Loránd University, Pázmány P. s. 1/C, Budapest 1117, Hungary, (email: takacsbm@caesar.elte.hu).

†MTA-ELTE Numerical Analysis and Large Networks Research Group, Eötvös Loránd University, Pázmány P. s. 1/C, Budapest 1117, Hungary, (email: hadjimy@cs.elte.hu).

The original models of Kermack and McKendric took into account constant rates of change and neglected any natural deaths and births or vaccination. In this work, we also consider constant rates of change and moreover we include a term that describes immunization effects through vaccination. Therefore, the original SIR model takes the following form:

$$\begin{cases} \frac{dS(t)}{dt} = -aS(t)I(t) - cS(t), \\ \frac{dI(t)}{dt} = aS(t)I(t) - bI(t), \\ \frac{dR(t)}{dt} = bI(t) + cS(t), \end{cases} \quad (1.1)$$

where the positive constant parameters a , b and c describe the rate of infection, recovery and vaccination, respectively.

Since the introduction of the model (1.1) in 1927, numerous extensions were constructed to describe biological processes more efficiently and realistically. One natural extension is to take into account the heterogeneity of our domain in a way that we examine not only the change of the populations in time, but also we observe the spatial movements. Such models were introduced by Kendall [12], in which they transformed the system of ordinary differential equations above into a system of partial differential equations.

Let us define a non-negative function $G(x, y, r, \theta)$ which describes an effect of a single point (x, y) in his δ -radius neighborhood $B_\delta(x, y)$, i.e. in which it can infect healthy individuals:

$$G(x, y, r, \theta) = \begin{cases} g_1(r)g_2(\theta), & \text{if } (x + \cos(\theta)r, y + \sin(\theta)r) \in B_\delta(x, y), \\ 0, & \text{otherwise.} \end{cases} \quad (1.2)$$

The function $G(x, y, r, \theta)$ describes the effect of the center point (x, y) at points $(x + r \cos(\theta), y + r \sin(\theta))$, in which $r \in [0, \delta]$ and $\theta \in [0, 2\pi]$ are polar coordinates, i.e., r is the distance from the center and θ is the angle. We suppose that $G(x, y, r, \theta)$ is separable, which is a natural assumption. The function describing the part of the effect depending on the distance from the center is $g_1(r)$, which is supposed to be non-negative, and also decreasing in a way that it takes zero for values $r \geq \delta$ (since we have an effect only inside our ball). The other function is $g_2(\theta)$, which characterizes the part of the effect depending on the angle, i.e. the direction in which the center is compared to point $(x + r \cos(\theta), y + r \sin(\theta))$. The case of constant function $g_2(\theta)$ is widely studied in [6] and [7], while a non-constant such function may be useful in the case of modeling the spread of diseases in a forest with a constant wind blowing in one direction which was described in [19]. In both cases it is supposed that the function is periodic in a way that $g_2(0) = g_2(2\pi)$.

Now let us examine the way we can rewrite equation (1.1) by using (1.2). The first equation takes the form

$$\frac{\partial S(t, x, y)}{\partial t} = -S(t, x, y) \int_0^\infty \int_0^{2\pi} G(x, y, r, \theta) I(t, \bar{x}(r, \theta), \bar{y}(r, \theta)) r d\theta dr - cS(t, x, y), \quad (1.3)$$

in which we used the notations $\bar{x}(r, \theta) = x + r \cos(\theta)$ and $\bar{y}(r, \theta) = y + r \sin(\theta)$. If we use the fact that $G(x, y, r, \theta) = 0$ outside the ball $B_\delta((x, y))$, then (1.3) can be rewritten as

$$\frac{\partial S(t, x, y)}{\partial t} = -S(t, x, y) \int_0^\delta \int_0^{2\pi} g_1(r)g_2(\theta)I(t, \bar{x}(r, \theta), \bar{y}(r, \theta)) r d\theta dr - cS(t, x, y). \quad (1.4)$$

The same procedure can be applied to the other two equations of (1.1) and consequently we get the following system of integro-differential equations:

$$\begin{cases} \frac{\partial S(t, x, y)}{\partial t} = -S(t, x, y) \int_0^\delta \int_0^{2\pi} g_1(r)g_2(\theta)I(t, \bar{x}(r, \theta), \bar{y}(r, \theta)) r d\theta dr - cS(t, x, y), \\ \frac{\partial I(t, x, y)}{\partial t} = S(t, x, y) \int_0^\delta \int_0^{2\pi} g_1(r)g_2(\theta)I(t, \bar{x}(r, \theta), \bar{y}(r, \theta)) r d\theta dr - bI(t, x, y), \\ \frac{\partial R(t, x, y)}{\partial t} = bI(t, x, y) + cS(t, x, y). \end{cases} \quad (1.5)$$

1.1 Outline and scope of the paper

The aim of this paper is twofold. First, in Section 2 we analyze the stability of the continuous model (1.1) and prove that a unique solution exists under some Lipschitz continuity and boundedness assumptions. Secondly, in Sections 3 and 4 we seek numerical schemes that approximate the solution of (1.1) and maintain its qualitative properties.

We verify that the exact solution satisfies biologically reasonable properties; however, due to its implicit form it cannot be used directly. A numerical approximation is presented in Section 2.2 that provably satisfies the solution's properties. The first order accuracy of this approximation motivates the search of suitable high order numerical methods that preserve a discrete analogue of the properties of the continuous model. In Section 3 we use cubature formulas to reduce the integro-differential system (1.5) to an ODE system. We study the accuracy of different cubatures and interpolation techniques for approximating the multiple integrals in (1.1). Furthermore, the employment of time integration methods yields an algebraic system to solve numerically. Section 4 shows that a step size restriction is sufficient and necessary such that the forward Euler method maintains the stability properties of the ODE system. We prove that high order strong-stability-preserving (SSP) Runge–Kutta methods can be used under appropriate restrictions; thus, we can obtain a high order stable scheme both in space and time. Finally in Section 5 we demonstrate the theoretical results by conducting numerical experiments.

2 Stability of the analytic solution

Analytic results for deterministic reaction epidemic models have been studied by several authors, see for example, [1, 12, 20]. Such models lie in the larger class of reaction-diffusion problems and therefore one can obtain theoretical results by studying the more general problem. We prove the uniqueness of solution of system (1.5) by following the work of Capasso and Fortunato [2].

We consider the following semilinear autonomous evolution problem

$$\begin{aligned}\frac{\partial u}{\partial t}(t) &= -Au(t) + F(u(t)) \\ u_0 &= u(0) \in D(A),\end{aligned}\tag{2.1}$$

where A be a self-adjoint positive operator in the real Hilbert space E with domain $D(A)$. Define $\lambda_0 = \inf \sigma(A)$, where $\sigma(A)$ denotes the spectrum of A . Let us choose $E := L^2(\Omega) \times L^2(\Omega)$ with scalar product $(\cdot|\cdot)$ and a norm defined by

$$\left\| \begin{pmatrix} u_1 \\ u_2 \end{pmatrix} \right\| = \left(\|u_1\|_{L^2}^2 + \|u_2\|_{L^2}^2 \right)^{\frac{1}{2}}.$$

We also equip $D(A)$ with the norm

$$\|u\|_A = \|Au\|, \quad u \in D(A).$$

In the view of problem (1.5), the linear operator is defined as

$$A \begin{pmatrix} u_1 \\ u_2 \end{pmatrix} := \begin{pmatrix} c & 0 \\ 0 & b \end{pmatrix} \begin{pmatrix} u_1 \\ u_2 \end{pmatrix}$$

It is easy to see that A is a self-adjoint and positive operator. We have

$$(Au, v) = \left(A \begin{pmatrix} u_1 \\ u_2 \end{pmatrix}, \begin{pmatrix} v_1 \\ v_2 \end{pmatrix} \right) = cu_1v_1 + bu_2v_2 = \left(\begin{pmatrix} u_1 \\ u_2 \end{pmatrix}, A \begin{pmatrix} v_1 \\ v_2 \end{pmatrix} \right) = (u, Av),$$

Also, parameters b and c are positive and hence

$$(Au, u) = cu_1^2 + bu_2^2 > 0.$$

Similarly, $F(u)$ consists of the nonlinear terms, and is defined as

$$F \begin{pmatrix} u_1 \\ u_2 \end{pmatrix} := \begin{pmatrix} -\mathcal{F}(u_1)u_2 \\ \mathcal{F}(u_1)u_2 \end{pmatrix}.\tag{2.2}$$

The function \mathcal{F} contains the integral part of (1.5) and is given by

$$\mathcal{F}(t, x, y) := \mathcal{F}(I(t, x, y)) = \int_0^\delta \int_0^{2\pi} g_1(r)g_2(\theta)I(t, \bar{x}(r, \theta), \bar{y}(r, \theta)) r \, d\theta dr.\tag{2.3}$$

Note that it is sufficient to consider only the first two equations in (1.5), since $R(t, x, y)$ can be obtained by using that the sum $S(t, x, y) + I(t, x, y) + R(t, x, y)$ is constant in time for every point (x, y) .

The main result of this section is Theorem 2.1 stating that a unique solution of system (1.5) exists. The proof of Theorem 2.1 relies on the fact that the function F in (2.1) is Lipschitz-continuous and bounded in $\|\cdot\|_A$. Therefore, we define the following conditions:

(A1) F is locally Lipschitz-continuous from $D(A)$ to $D(A)$, i.e.

$$\|F(u) - F(v)\|_A \leq c(d) \|u - v\|_A$$

for all $u, v \in D(A)$ such that $\|u\|_A, \|v\|_A \leq d, d \geq 0$.

(A2) Let us assume that $k, \gamma \geq 0$ exists such that

$$\|F(u)\|_A \leq k \|u\|_A^{1+\gamma}, \quad \forall u \in D(A)$$

Theorem 2.1. *Consider the problem (1.5) and assume that conditions (A1) and (A2) hold. Then, a unique strong solution of system (1.5) exists on some interval $[0, T[$. Moreover, if the initial condition $u_0 \in K$, where*

$$K = \left\{ u \in L^2(\Omega) \left| \|u\|_A < \frac{\min(b, c)}{\sqrt{2\kappa_1\kappa_2} \mu(\Omega)} \right. \right\},$$

then the zero solution is the unique equilibrium solution of (1.5).

The proof of Theorem 2.1 is a direct consequence of Theorem 1.1 and Theorem 1.3 in [2]. For clarity, we state these two theorems below.

Theorem 2.2. [2, Theorem 1.1] *Assume that condition (A1) holds. Then a unique strong solution of problem (2.1) exists in some interval $[0, T[$.*

Theorem 2.3. [2, Theorem 1.3] *Assume that conditions (A1) and (A2) hold. Then for any $u_0 \in K$ a global strong solution $u(t)$ in $D(A)$ of (2.1) exists, i.e., $u \in C^1(]0, T[, E) \cap C([0, T[, D(A))$. Moreover, the zero solution is asymptotically stable in K . Here*

$$K = \begin{cases} \{u \in D(A) \mid \|u\|_A < (\lambda_0/k)^{1/\gamma}\} & \text{if } \gamma > 0, \\ D(A) & \text{if } \gamma = 0 \text{ and } \lambda_0 > k. \end{cases}$$

In the rest of the section we show that the function F as defined in (2.2) satisfies the conditions (A1) and (A2). We first prove some necessary lemmas.

Lemma 2.1. *The norms $\|\cdot\|$ and $\|\cdot\|_A$ are equivalent, i.e.,*

$$\|u\| \leq \max\left(\frac{1}{c}, \frac{1}{b}\right) \|u\|_A \quad \text{and} \quad \|u\|_A \leq \max(c, b) \|u\|$$

Proof. The proof is the following straightforward calculations:

$$\begin{aligned} \|u\|_A^2 &= c^2 \|u_1\|^2 + b^2 \|u_2\|^2 \leq \max(c^2, b^2) (\|u_1\|^2 + \|u_2\|^2) = \max(c^2, b^2) \|u\|^2 \\ \|u\|^2 &= c^2 \frac{1}{c^2} \|u_1\|^2 + b^2 \frac{1}{b^2} \|u_2\|^2 \leq \max\left(\frac{1}{c^2}, \frac{1}{b^2}\right) (c^2 \|u_1\|^2 + b^2 \|u_2\|^2) = \max\left(\frac{1}{c^2}, \frac{1}{b^2}\right) \|u\|_A^2. \end{aligned}$$

□

Lemma 2.2. *The following holds for \mathcal{F} :*

$$\|\mathcal{F}(u)\|_{L^2} \leq k_{\mathcal{F}} \|u\|_{L^2}$$

Proof. The term we are going to give an upper bound to is

$$\begin{aligned} \|\mathcal{F}(I)\|_{L^2}^2 &= \int_{\Omega} \left| \int_0^{\delta} \int_0^{2\pi} g_1(r) g_2(\theta) I(t, \bar{x}(r, \theta), \bar{y}(r, \theta)) r \, d\theta dr \right|^2 dx dy \\ &= \int_{\Omega} \left| \int_{B_{\delta}(\mathbf{x})} g_1(r) g_2(\theta) I(t, \bar{\mathbf{x}}) \, d\bar{\mathbf{x}} \right|^2 d\mathbf{x}, \end{aligned}$$

in which we used the notation $\mathbf{x} := (x, y)$ and $B_{\delta}(\mathbf{x})$ is the ball with radius δ around \mathbf{x} . By the definition of g_1 and g_2 :

$$\|\mathcal{F}(I)\|_{L^2}^2 = \int_{\Omega} \left| \int_{\Omega} g_1(r) g_2(\theta) I(t, \bar{\mathbf{x}}) \, d\bar{\mathbf{x}} \right|^2 d\mathbf{x}.$$

By definition, we know that g_1 and g_2 are bounded. Let us use the notations $\kappa_1 = \max_{r \in (0, \delta)} \{g_1(r)\}$ and $\kappa_2 = \max_{\theta \in (0, 2\pi)} \{g_2(\theta)\}$. Then,

$$\begin{aligned} \|\mathcal{F}(I)\|_{L^2}^2 &\leq \kappa_1^2 \kappa_2^2 \int_{\Omega} \left| \int_{\Omega} I(t, \bar{\mathbf{x}}) \, d\bar{\mathbf{x}} \right|^2 d\mathbf{x} = \kappa_1^2 \kappa_2^2 \int_{\Omega} \left| \int_{\Omega} 1 \cdot I(t, \bar{\mathbf{x}}) \, d\bar{\mathbf{x}} \right|^2 d\mathbf{x} \\ &\leq \kappa_1^2 \kappa_2^2 \int_{\Omega} \left| \sqrt{\int_{\Omega} 1^2 d\bar{\mathbf{x}}} \sqrt{\int_{\Omega} (I(t, \bar{\mathbf{x}}))^2 d\bar{\mathbf{x}}} \right|^2 d\mathbf{x} \\ &\leq \kappa_1^2 \kappa_2^2 \mu(\Omega) \int_{\Omega} \int_{\Omega} |I(t, \bar{\mathbf{x}})|^2 d\bar{\mathbf{x}} d\mathbf{x}, \end{aligned}$$

in which we used the Cauchy-Schwartz inequality, and $\mu(\Omega)$ is the Lebesgue-measure of Ω . It holds that

$$\int_{\Omega} \int_{\Omega} |I(t, \bar{\mathbf{x}})|^2 d\bar{\mathbf{x}} d\mathbf{x} = \int_{\Omega} \|I\|_{L^2}^2 d\mathbf{x} = \mu(\Omega) \|I\|_{L^2}^2.$$

Consequently,

$$\|\mathcal{F}(I)\|_{L^2} \leq \kappa_1 \kappa_2 \mu(\Omega) \|I\|_{L^2},$$

from which we get that $k_{\mathcal{F}} = \kappa_1 \kappa_2 \mu(\Omega)$. □

Corollary 2.1. *Consider F given by (2.2). Then, condition (A2) holds with $\gamma = 1$.*

Proof. Because of Lemma 2.1, it is enough to prove

$$\|F(u)\| \leq k \|u\|^2, \tag{2.4}$$

since from this we get

$$\|F(u)\|_A \leq \max(c, b) \|F(u)\| \leq \max(c, b) k \|u\|^2 \leq \max(c, b) \max\left(\frac{1}{c}, \frac{1}{b}\right) k \|u\|_A^2.$$

Inequality (2.4) can be proved the following way:

$$\begin{aligned} \|F(u)\| &= \left\| \begin{pmatrix} -\mathcal{F}(u_1)u_2 \\ \mathcal{F}(u_1)u_2 \end{pmatrix} \right\| = (\|\mathcal{F}(u_1)u_2\|_{L^2}^2 + \|\mathcal{F}(u_1)u_2\|_{L^2}^2)^{1/2} \\ &\leq \sqrt{2} \|\mathcal{F}(u_1)\|_{L^2} \|u_2\|_{L^2} \\ &\leq \sqrt{2}k_{\mathcal{F}} \|u_1\|_{L^2} \|u_2\|_{L^2}. \end{aligned}$$

Using Lemma 2.2 we have

$$\|u_1\|_{L^2} \|u_2\|_{L^2} \leq \|u_1\|_{L^2}^2 + \|u_2\|_{L^2}^2 = \|u\|^2,$$

which means that $k = \sqrt{2}k_{\mathcal{F}} = \sqrt{2}\kappa_1\kappa_2 \mu(\Omega)$. □

Lemma 2.3. Consider \mathcal{F} given by (2.3). Then, the following condition holds:

$$\|\mathcal{F}(u) - \mathcal{F}(v)\|_{L^2} \leq C_{\mathcal{F}} \|u - v\|_{L^2}.$$

Proof. We would like to bound the following expression:

$$\begin{aligned} &\|\mathcal{F}(I_1) - \mathcal{F}(I_2)\|_{L^2}^2 = \\ &\int_{\Omega} \left| \int_0^{\delta} \int_0^{2\pi} g_1(r)g_2(\theta) (I_1(t, \bar{x}(r, \theta), \bar{y}(r, \theta)) - I_2(t, \bar{x}(r, \theta), \bar{y}(r, \theta))) r d\theta dr \right|^2 dx dy. \end{aligned}$$

We can proceed similarly as in the proof of Lemma 2.2:

$$\begin{aligned} \|\mathcal{F}(I_1) - \mathcal{F}(I_2)\|_{L^2}^2 &= \int_{\Omega} \left| \int_{B_{\delta}(\mathbf{x})} g_1(r)g_2(\theta) (I_1(t, \bar{\mathbf{x}}) - I_2(t, \bar{\mathbf{x}})) d\bar{\mathbf{x}} \right|^2 d\mathbf{x} \\ &= \int_{\Omega} \left| \int_{\Omega} g_1(r)g_2(\theta) (I_1(t, \bar{\mathbf{x}}) - I_2(t, \bar{\mathbf{x}})) d\bar{\mathbf{x}} \right|^2 d\mathbf{x} \\ &\leq \kappa_1^2 \kappa_2^2 \int_{\Omega} \left| \int_{\Omega} (I_1(t, \bar{\mathbf{x}}) - I_2(t, \bar{\mathbf{x}})) d\bar{\mathbf{x}} \right|^2 d\mathbf{x} \\ &\leq \kappa_1^2 \kappa_2^2 \mu(\Omega) \int_{\Omega} \int_{\Omega} |I_1(t, \bar{\mathbf{x}}) - I_2(t, \bar{\mathbf{x}})|^2 d\bar{\mathbf{x}} d\mathbf{x} \\ &= \kappa_1^2 \kappa_2^2 \mu(\Omega) \int_{\Omega} \|I_1 - I_2\|_{L^2}^2 d\mathbf{x} \\ &= \kappa_1^2 \kappa_2^2 \mu(\Omega)^2 \|I_1 - I_2\|_{L^2}^2. \end{aligned}$$

which completes the proof with $C_{\mathcal{F}} = \kappa_1\kappa_2 \mu(\Omega)$. □

Lemma 2.4. Consider F given by (2.2). Then, condition (A1) holds.

Proof. Because of Lemma 2.1, it is enough to prove

$$\|F(u) - F(v)\| \leq k \|u - v\|. \tag{2.5}$$

If (2.5) holds, then

$$\begin{aligned}\|F(u) - F(v)\|_A &\leq \max(c, b) \|F(u) - F(v)\| \\ &\leq \max(c, b) k \|u - v\| \\ &\leq \max(c, b) \max\left(\frac{1}{c}, \frac{1}{b}\right) k \|u - v\|_A.\end{aligned}$$

For inequality (2.5), we get the following calculations:

$$\begin{aligned}\|F(u) - F(v)\| &= \left\| \begin{pmatrix} -\mathcal{F}(u_1)u_2 + \mathcal{F}(v_1)v_2 \\ \mathcal{F}(u_1)u_2 - \mathcal{F}(v_1)v_2 \end{pmatrix} \right\| \\ &\leq (\|\mathcal{F}(u_1)u_2 - \mathcal{F}(v_1)v_2\|_{L^2}^2 + \|\mathcal{F}(u_1)u_2 - \mathcal{F}(v_1)v_2\|_{L^2}^2)^{1/2}.\end{aligned}$$

Now we use the following estimation:

$$\|\mathcal{F}(u_1)u_2 - \mathcal{F}(v_1)v_2\|_{L^2}^2 = \|\mathcal{F}(u_1)u_2 - \mathcal{F}(u_1)v_2 + \mathcal{F}(u_1)v_2 - \mathcal{F}(v_1)v_2\|_{L^2}^2 \quad (2.6)$$

$$\leq \|\mathcal{F}(u_1)u_2 - \mathcal{F}(u_1)v_2\|_{L^2}^2 + \|\mathcal{F}(u_1)v_2 - \mathcal{F}(v_1)v_2\|_{L^2}^2 \quad (2.7)$$

$$= \|\mathcal{F}(u_1)\|^2 \|u_2 - v_2\|_{L^2}^2 + \|\mathcal{F}(u_1) - \mathcal{F}(v_1)\|_{L^2}^2 \|v_2\|_{L^2}^2. \quad (2.8)$$

Lemma 2.2 yields

$$\|\mathcal{F}(u_1)\|^2 \|u_2 - v_2\|_{L^2}^2 \leq k_{\mathcal{F}}^2 d^4 \|u_2 - v_2\|_{L^2}^2$$

and by using the fact that $\|v_2\| \leq d$ we can bound (2.6) to get

$$\|\mathcal{F}(u_1)u_2 - \mathcal{F}(v_1)v_2\|_{L^2}^2 \leq k_{\mathcal{F}}^2 d^4 \|u_2 - v_2\|_{L^2}^2 + \|\mathcal{F}(u_1) - \mathcal{F}(v_1)\|_{L^2}^2 d^2.$$

From Lemma 2.3 we also have

$$\|\mathcal{F}(u_1) - \mathcal{F}(v_1)\|_{L^2}^2 d^2 \leq C_{\mathcal{F}}^2 \|u_1 - v_1\|_{L^2}^2 d^2 \quad (2.9)$$

Putting all together, we get

$$\begin{aligned}\|F(u) - F(v)\| &\leq \sqrt{2} \|\mathcal{F}(u_1)u_2 - \mathcal{F}(v_1)v_2\|_{L^2} \\ &\leq \sqrt{2} (k_{\mathcal{F}}^2 d^4 \|u_2 - v_2\|_{L^2}^2 + C_{\mathcal{F}}^2 d^2 \|u_1 - v_1\|_{L^2}^2)^{1/2} \\ &\leq \sqrt{2} \max(k_{\mathcal{F}} d^2, C_{\mathcal{F}} d) \|u - v\|,\end{aligned}$$

which completes the proof with Lipschitz constant

$$\begin{aligned}c(d) &= \sqrt{2} \max(c, b) \max\left(\frac{1}{c}, \frac{1}{b}\right) \max(k_{\mathcal{F}} d^2, C_{\mathcal{F}} d) \\ &= \sqrt{2} \kappa_1 \kappa_2 \mu(\Omega) \max(c, b) \max\left(\frac{1}{c}, \frac{1}{b}\right) \max(d^2, d),\end{aligned}$$

where we used the fact that $k_{\mathcal{F}} = C_{\mathcal{F}} = \kappa_1 \kappa_2 \mu(\Omega)$. \square

Corollary 2.1 and Lemma 2.4 show that function (2.2) satisfies conditions (A1) and (A2). We know from Lemma 2.1 that $\gamma = 1$, so we define the set K by using

$$\left(\frac{\lambda_0}{k}\right)^{\frac{1}{\gamma}} = \frac{\min(b, c)}{\sqrt{2} \kappa_1 \kappa_2 \mu(\Omega)}.$$

Therefore, the proof of Theorem 2.1 follows from Theorem 2.2 and Theorem 2.3.

2.1 Qualitative behavior of the model

When deriving a mathematical model to describe the spread of an epidemic in both space and time, it is essential that the real-life processes are being represented as accurately as possible. More precisely, numerical discretizations applied to such models should preserve the qualitative properties of the original epidemic model.

The first, and perhaps most natural property is that the number of each species is non-negative at every time and point of the domain. Because in our models we use densities, this property can be formulated as follows:

C_1 : The densities $X(t, x, y)$ ($X \in \{S, I, R\}$) are non-negative at every point $(x, y) \in \Omega$.

Assuming that the births and natural deaths are the same (vital dynamics have no effect on the process), the total number of species (the sum of the species of each classes) should not increase nor decrease. Thus we have the following property:

C_2 : The sum $S(t, x, y) + I(t, x, y) + R(t, x, y)$ should be constant in time for every $(x, y) \in \Omega$, i.e.,

$$\int_{\Omega} S(t, x, y) + I(t, x, y) + R(t, x, y) \, dx \, dy = \text{const}, \quad \forall t.$$

Another property concerns the number of susceptibles: since an individual gets to the recovered class after the infection, the number of susceptibles cannot increase in time. In mathematical terms:

C_3 : Function $S(t, x, y)$ is non-increasing in time at every (x, y) .

Similarly, the number of recovered species cannot decrease in time, thus:

C_4 : Function $R(t, x, y)$ is non-increasing in t at every $(x, y) \in \Omega$.

As in the previous section, instead of proving the preservation of properties $C_1 - C_4$ for the particular model (1.5), we can establish theoretical results for a more general system of equations. First, we prove the following lemma.

Lemma 2.5. *The solution of (1.5) depends continuously on the right hand side of the equation.*

Proof. The proof uses the method of variation of constants. Consider the nonhomogeneous semilinear equation

$$u'(t) = Au(t) + F(u(t)), \tag{2.10}$$

where A is a linear bounded operator and F is Hölder continuous. Then, the solution corresponds of the solution of the following integral equation:

$$u(t) = \mathcal{S}(t)u_0 + \int_0^t \mathcal{S}(t-s)F(s)ds, \tag{2.11}$$

where $\mathcal{S}(t)$ is the analytic semigroup associated with the infinitesimal generator A .

For the system (1.5) we use similar choices as in the beginning of this section, namely

$$A \begin{pmatrix} u_1 \\ u_2 \end{pmatrix} = \begin{pmatrix} c & 0 \\ 0 & b \end{pmatrix} \begin{pmatrix} u_1 \\ u_2 \end{pmatrix}$$

and

$$F_\varepsilon \begin{pmatrix} u_1 \\ u_2 \end{pmatrix} = \begin{pmatrix} -\mathcal{F}(u_1)u_2 \\ \mathcal{F}(u_1)u_2 + \varepsilon \end{pmatrix}, \quad (2.12)$$

where $\mathcal{F}(u)$ is given by (2.3). Note that we do not consider the third equation of (1.5), since as noted before it can be omitted.

It is clear that A generates an analytical semigroup, and we also know that F is Lipschitz-continuous because of Lemma 2.4; hence, the method of variation of constants is applicable. Consequently, if u_{ε_1} and u_{ε_2} are solutions of (2.11), then

$$\|u_{\varepsilon_1} - u_{\varepsilon_2}\| = \left\| \mathcal{S}(t)u_0 + \int_0^t \mathcal{S}(t-s)F_{\varepsilon_1}(s)ds - \mathcal{S}(t)u_0 - \int_0^t \mathcal{S}(t-s)F_{\varepsilon_2}(s)ds \right\|.$$

Using (2.2), we can express (2.12) as

$$F_\varepsilon \begin{pmatrix} u_1 \\ u_2 \end{pmatrix} = F \begin{pmatrix} u_1 \\ u_2 \end{pmatrix} + \begin{pmatrix} 0 \\ \varepsilon \end{pmatrix}.$$

Let $\tilde{\varepsilon} = (0 \ \varepsilon)^\top$, then

$$\|u_{\varepsilon_1} - u_{\varepsilon_2}\| = \left\| \int_0^t \mathcal{S}(t-s)(F(s) + \tilde{\varepsilon}_1 - F(s) - \tilde{\varepsilon}_2)ds \right\| = \left\| (\tilde{\varepsilon}_1 - \tilde{\varepsilon}_2) \int_0^t \mathcal{S}(t-s)ds \right\|.$$

As both ε_1 and ε_2 tend to zero, then the above expression tends to zero too, and this completes the proof. \square

Lemma 2.5 facilitates the proof of the next theorem.

Theorem 2.4. *Consider the following system of equations*

$$\begin{cases} \frac{\partial S(t, x, y)}{\partial t} = -S(t, x, y)H(\mathcal{B}(I(t, x, y))) - cS(t, x, y), \\ \frac{\partial I(t, x, y)}{\partial t} = S(t, x, y)H(\mathcal{B}(I(t, x, y))) - bI(t, x, y), \\ \frac{\partial R(t, x, y)}{\partial t} = bI(t, x, y), \end{cases} \quad (2.13)$$

where $\mathcal{B}(I(t, x, y)) := \{I(t, \tilde{x}, \tilde{y}) : (\tilde{x}, \tilde{y}) \in \mathcal{D}_{(x, y)} \subset \mathbb{R}^2\}$ and $H : \mathbb{R} \rightarrow \mathbb{R}$ is a continuous operator. Suppose that H is non-negative in the sense that if $\mathcal{D}_0^+ \subset \mathbb{R}_0^+$, ($\mathbb{R}_0^+ = \mathbb{R}^+ \cup \{0\}$), then $H(\mathcal{D}_0^+) \geq 0$. In this case the properties $C_1 - C_4$ hold without any restriction on the time interval $t \in [0, t_f]$.

Proof. First we prove the non-negativity of $I(t, x, y)$. For this, let us consider a modified version of (2.13):

$$\begin{cases} \frac{\partial S_\varepsilon(t, x, y)}{\partial t} = -S_\varepsilon(t, x, y)H(\mathcal{B}(I_\varepsilon(t, x, y))) - cS_\varepsilon(t, x, y), \\ \frac{\partial I_\varepsilon(t, x, y)}{\partial t} = S_\varepsilon(t, x, y)H(\mathcal{B}(I_\varepsilon(t, x, y))) - bI_\varepsilon(t, x, y) + \varepsilon, \\ \frac{\partial R_\varepsilon(t, x, y)}{\partial t} = bI_\varepsilon(t, x, y), \end{cases} \quad (2.14)$$

where $\varepsilon : \mathbb{R} \rightarrow \mathbb{R}$ is a constant positive function.

Let us define by t_0 the first moment in time such that $I_\varepsilon(t, x, y)$ takes negative values, i.e.,

$$t_0 := \inf\{t \mid \exists(x, y) \in \Omega : I_\varepsilon(t, x, y) < 0\}.$$

This t_0 exists because of the non-negativity of our initial conditions, and the continuity of function I_ε . Because of this latter property and the definition of t_0 , there is a point (x_0, y_0) for which $I_\varepsilon(t_0, x_0, y_0) = 0$, and

$$\frac{\partial I_\varepsilon(t_0, x_0, y_0)}{\partial t} \leq 0. \quad (2.15)$$

We also know that $H(\mathcal{B}(I_\varepsilon(t_0, x, y))) \geq 0$ (since I_ε is non-negative at t_0).

However, if we look at the second equation in (2.14), we can see that the second term is zero, so the term $S_\varepsilon(t_0, x_0, y_0)H(\mathcal{B}(I_\varepsilon(t_0, x, y)))$ must be negative for condition (2.15) to hold (since ε is positive).

Let us divide the first equation of (2.14) by S , and integrate it with respect to time t from 0 to t_0 . In this way we obtain

$$\log(S_\varepsilon(t_0, x, y)) - \log(S_\varepsilon(0, x, y)) = - \int_0^{t_0} H(\mathcal{B}(I_\varepsilon(t_0, x, y))) dt - ct.$$

By reformulating, we get

$$S_\varepsilon(t_0, x_0, y_0) = S_\varepsilon(0, x_0, y_0) \exp\left(- \int_0^{t_0} H(\mathcal{B}(I_\varepsilon(t_0, x, y))) dt - ct\right). \quad (2.16)$$

Therefore $S_\varepsilon(t_0, x_0, y_0)$ is nonnegative, and we can also see that it is non-increasing. Adding ε to the two previously described terms we get that the derivative is positive, meaning that I_ε is nonnegative, which gives the contradiction. In this way $I_\varepsilon(t_0, x, y) \geq 0$ for every $t \in [0, t_f]$ and (x, y) . Consequently, since $R(0, x, y)$ is non-negative, we get the non-decreasing and also the positivity of $R(t, x, y)$. In this way we proved that the solution of 2.14 satisfies $C_1 - C_4$.

We also know that because of continuous dependence by Lemma 2.5,

$$\lim_{\varepsilon \rightarrow 0} X_\varepsilon(t, x, y) \Big|_{t \in [0, t_f]} - X(t, x, y) \Big|_{t \in [0, t_f]} = 0,$$

for every $X \in \{S, I, R\}$. Therefore, properties $C_1 - C_4$ are satisfied by the solution of system (2.13). \square

Due to the complicated form of these equations one can suspect that no analytical solution can be derived for system (1.5). Because of this, we are going to use numerical methods to solve these equations.

However, the analytic solution of the original SIR model (1.1) has been recently described in the papers by Harko et al. [9] and Miller [16], [17]. Thus, we can get similar results applying their observations to our modified model (1.5). The analytic solution of system (1.5) can be written as

$$\begin{cases} S(t, x, y) = S(0, x, y)e^{-\xi(t, x, y) - ct}, \\ I(t, x, y) = M_0(x, y) - S(t, x, y) - R(t, x, y), \\ R(t, x, y) = R(0, x, y) + b \int_0^t I(s, x, y) ds + c \int_0^t S(s, x, y) ds, \end{cases} \quad (2.17)$$

where we use the notations

$$\begin{aligned} M_0(x, y) &:= S(0, x, y) + I(0, x, y) + R(0, x, y), \\ \xi(t, x, y) &:= \int_0^t \mathcal{F}(s, x, y) ds, \end{aligned}$$

and \mathcal{F} is given by (2.3).

It is evident that in (2.17), the values of the functions at a given time t^* can only be computed if the values in the interval $[0, t^*)$ are known. Consequently, these formulas are not useful in the practical sense, but will be used later in the proof of the convergence of our numerical methods.

Since the values of the functions cannot be calculated directly, numerical methods are needed to approximate them. We can take two possible paths:

1. We can approximate the values of $\xi(t, x, y)$ by numerical integration.
2. We can solve the original equation (1.5) by a numerical method.

The first approach is discussed in Section 2.2, while the rest of the papers considers the second case. We not only focus on the order and convergence of our numerical methods, but also check whether the qualitative properties $C_1 - C_4$ of the analytic solution are preserved by the numerical method or not. Therefore, we denote the discrete versions of conditions $C_1 - C_4$ by $D_1 - D_4$.

2.2 Numerical approximation of the integral solution

As noted before, if we would like to use the solution (2.17), we have to approximate the involved integrals. This can be achieved by splitting our time interval $[0, t_f]$ into smaller sections using a constant step size τ . By taking this approach, the integrals can be approximated by a left Riemann sum, taking the values in each section at the left endpoint, i.e., in the case of the integral of I :

$$\int_0^{(n+1)\tau} I(s, x, y) ds \approx \tau \sum_{k=0}^n I(k\tau, x, y).$$

Another important observation is that the integral equations can be rewritten in a recursive form:

$$\begin{cases} S((n+1)\tau, x, y) = S(n\tau, x, y) \exp\left(-\int_{n\tau}^{(n+1)\tau} \mathcal{F}(s, x, y) ds - c\tau\right), \\ R((n+1)\tau, x, y) = R(n\tau, x, y) + b \int_{n\tau}^{(n+1)\tau} I(s, x, y) ds + c \int_{n\tau}^{(n+1)\tau} S(s, x, y) ds, \\ I((n+1)\tau, x, y) = M_0(x, y) - S((n+1)\tau, x, y) - R((n+1)\tau, x, y). \end{cases} \quad (2.18)$$

Taking these into account, we let $X^n := X^n(x, y)$ to be an approximation of the function $X(n\tau, x, y)$, $X \in \{S, I, R, \mathcal{F}\}$. Then, we can write the following scheme:

$$\begin{cases} S^{n+1} = S^n e^{-\tau \mathcal{F}^n - c\tau}, \\ R^{n+1} = R^n + b\tau I^n + c\tau S^{n+1}, \\ I^{n+1} = (S^0 + I^0 + R^0) - S^{n+1} - R^{n+1}, \end{cases} \quad (2.19)$$

where we choose to approximate $\int_{n\tau}^{(n+1)\tau} S(s, x, y) ds$ by τS^{n+1} . Note that in this case the order of the equations in (2.19) is important as estimates at time t_{n+1} are used to update the rest of solution's components.

Theorem 2.5. *The solution of the scheme (2.19) satisfies properties $D_1 - D_4$, if $0 < \tau \leq 1/b$.*

Proof. We prove the statement by induction. By adding up the equations we get D_2 . It is also easy to see that property D_3 and D_4 holds, since the argument $-\tau \mathcal{F}^n - c\tau$ is negative, and the right hand side terms of the rule of R^{n+1} are positive. Also, D_1 is true for S and R because of the same reasons.

Assume that at the n th-step the solution satisfies properties $D_1 - D_4$. From (2.19) we have

$$\begin{aligned} I^{n+1} &= (S^0 + I^0 + R^0) - S^{n+1} - R^{n+1} \\ &= (S^n + I^n + R^n) - S^{n+1} - R^{n+1} \\ &= S^n \left(1 - (1 + c\tau)e^{-\tau(\mathcal{F}^n + c)}\right) + I^n (1 - b\tau). \end{aligned}$$

By assumption, S^n and I^n are non-negative, thus a sufficient condition for I^{n+1} to be non-negative is

$$1 - (1 + c\tau)e^{-\tau(\mathcal{F}^n + c)} \geq 0 \quad \text{and} \quad 1 - b\tau \geq 0.$$

Note that $x - \ln(1 + x) \geq 0$ for any real-value number $x > -1$. Since $c \geq 0$ and \mathcal{F}^n is non-negative we then have $\tau \mathcal{F}^n + c\tau - \ln(1 + c\tau) \geq 0$. Rearranging the inequality gives

$$\ln\left(\frac{1}{1 + c\tau}\right) \geq -\tau(\mathcal{F}^n + c),$$

hence $1 - (1 + c\tau)e^{-\tau(\mathcal{F}^n + c)} \geq 0$ for any $\tau > 0$. As a result, a sufficient condition for I^n to remain non-negative is $0 < \tau \leq 1/b$. \square

Remark 2.1. Using left Riemann sums to approximate the integrals in (2.18) results in local errors of order $\mathcal{O}(\tau^2)$. Therefore, the solution of (2.18) can only be first order accurate.

In the next two sections, we discretize (1.5) by first using a numerical approximation of the integral of the right hand side of the system, and then applying a time integration method. This approach results in numerical schemes that are high-order accurate, both in space and time.

3 Spatial discretisation

It is evident that the key point of the numerical solution of problem (1.5) is the approximation of $\mathcal{F}(t, x, y)$. This can be done in two different ways: one of them is to approximate the function $I(t, \bar{x}(r, \theta), \bar{y}(r, \theta))$ by a Taylor expansion, and then proceed further. This method is studied in [6] and [7], but is not efficient in the case of non-constant function $g_2(\theta)$ as shown in [19]. The other approach is to use a combination of interpolation and numerical integration (by using cubature formulas) to obtain an approximation of $\mathcal{F}(t, x, y)$.

We consider a two dimensional cubature formulas on the disc of radius δ with positive coefficients. Let the set of cubature points denoted by $\mathcal{Q}(x, y)$ in the disk $B_\delta(x, y)$ parametrized by polar coordinates (see [19])

$$\mathcal{Q}(x, y) := \{(x + r_i \cos(\theta_j), y + r_i \sin(\theta_j)) \in \text{Int}(B_\delta(x, y)), i \in \mathcal{I}, j \in \mathcal{J}\},$$

where r_i denotes the distance from center point (x, y) , θ_j is the angle, and \mathcal{I} and \mathcal{J} are the set of indices of cubature points. Using numerical integration, we get the following system:

$$\begin{cases} \frac{\partial S(t, x, y)}{\partial t} = -S(t, x, y)T(t, \mathcal{Q}(x, y)) - cS(t, x, y), \\ \frac{\partial I(t, x, y)}{\partial t} = S(t, x, y)T(t, \mathcal{Q}(x, y)) - bI(t, x, y), \\ \frac{\partial R(t, x, y)}{\partial t} = bI(t, x, y) + cS(t, x, y), \end{cases} \quad (3.1)$$

where

$$T(t, \mathcal{Q}(x, y)) = \sum_{(x_{i,j}, y_{i,j}) \in \mathcal{Q}(x, y)} w_{i,j} g_1(r_i) g_2(\theta_j) I(t, x + r_i \cos(\theta_j), y + r_i \sin(\theta_j)).$$

Remark 3.1. Note that Theorem 2.4 can be applied to this system (3.1); hence, the properties $C_1 - C_4$ hold without any restrictions for the solution of this system. Moreover, it can be easily shown that $T(t, \mathcal{Q}(x, y))$ satisfies properties (A1) and (A2), by following the proofs of Lemma 2.2 and Lemma 2.3. As a result a unique strong solution for system (3.1) exists.

3.1 Semi-discretization

Now we would like to solve (3.1) numerically. The first step is to discretize the problem in space. Let us suppose that we would like to solve our problem on a rectangle-shaped domain,

namely $\Omega := [0, A] \times [0, B]$. For our numerical solutions we will discretize this domain by using a spatial grid

$$\mathcal{G} := \{(x_k, y_l) \in \Omega \mid 1 \leq k \leq K, 1 \leq l \leq L\},$$

which consists of $K \times L$ points with spatial step sizes h_1 and h_2 , and approximate the continuous solutions by a vector of the values at the gridpoints.

After this semi-discretisation, we get the following set of equations

$$\begin{cases} \frac{dS_{k,l}(t)}{dt} = -S_{k,l}(t)T_{k,l}(t, \mathcal{Q}(x_k, y_l)) - cS_{k,l}(t), \\ \frac{dI_{k,l}(t)}{dt} = S_{k,l}(t)T_{k,l}(t, \mathcal{Q}(x_k, y_l)) - bI_{k,l}(t), \\ \frac{dR_{k,l}(t)}{dt} = bI_{k,l}(t) + cS_{k,l}(t), \end{cases} \quad (3.2)$$

where $X_{k,l}(t)$, $X \in \{S, I, R\}$, denotes the approximation of the function at gridpoint (x_k, y_l) , and $T_{k,l}(t, \mathcal{Q}(x_k, y_l))$ is the approximation of $\mathcal{F}(\cdot, x_k, y_l)$, defined in the following way:

$$T_{k,l}(t, \mathcal{Q}(x_k, y_l)) := \sum_{(x_{i,j}, y_{i,j}) \in \mathcal{Q}(x_k, y_l)} w_{i,j} g_1(r_i) g_2(\theta_j) \tilde{I}(t, x_k + r_i \cos(\theta_j), y_l + r_i \sin(\theta_j)). \quad (3.3)$$

Note that the points $(x_k + r_i \cos(\theta_j), y_l + r_i \sin(\theta_j))$ might not be part of \mathcal{G} , so there are no $I_{k,l}$ values assigned to them. Because of this, we will approximate them by a positivity preserving interpolation (e.g. bilinear) using the nearest known $I_{k,l}$ values and positive coefficients. This is the why \tilde{I} is used in (3.3) instead of I .

Theorem 3.1. *A unique strong solution for system (3.2) exists, for which properties $C_1 - C_4$ hold without any restrictions locally at a given point (x_k, y_l) .*

Proof. The proof of existence and uniqueness comes from the Lipschitz continuity and boundness of the right hand side, which can be proved similarly as in Corollary 2.1 and Lemma 2.4. Properties $C_1 - C_4$ can be proved in a similar manner as in Theorem 2.4. \square

The next theorem characterizes the accuracy of interpolation and cubature techniques of system (3.2).

Theorem 3.2. *Suppose that a cubature rule approximates the integral to order p , i.e.,*

$$\|\mathcal{F}(u) - T(t, \mathcal{Q}(x, y))\| = O(\delta^p),$$

where δ is the radius of the disk in which the integration takes place. Let us suppose that our (positivity preserving) interpolation approximates the values of I in order q , i.e.

$$\|I - \tilde{I}\| = O(h^q)$$

where h is the spatial step size. Then if u is the solution of (1.5) and v is the solution of (3.2), then

$$\|u - v\| = O(\delta^p) + O(h^q).$$

Proof. Let us proceed in two steps: first prove that if we w is the solution of (3.1), then

$$\|u - w\| = O(\delta^p) \quad \text{and} \quad \|w - v\| = O(h^q)$$

We prove both statements similarly as Lemma 2.5, namely by applying the formula of constant variations.

$$\begin{aligned} \|u - w\| &= \left\| S(t)u_0 + \int_0^t S(t-s)F(s)ds - S(t)u_0 - \int_0^t S(t-s)(F(s) + O(\delta^p)) \right\| \\ &= \left\| \int_0^t S(t-s)O(\delta^p) \right\| = O(\delta^p). \end{aligned}$$

The second one is also similar:

$$\begin{aligned} \|w - v\| &= \left\| S(t)u_0 + \int_0^t S(t-s)F(s)ds - S(t)u_0 - \int_0^t S(t-s)(F(s) + O(h^q)) \right\| \\ &= \left\| \int_0^t S(t-s)O(h^q) \right\| = O(h^q). \end{aligned}$$

□

A natural question is the type of cubature and interpolation to use in (3.2). In the case of cubature rules, we can choose two types of cubatures: a uniform and a nonuniform one.

3.1.1 Uniform cubature

We can use a direct cubature rule on the general disk, see for example [3, 18]. In such case the integral of a function $f(x, y)$ over the disk with radius δ can be approximated by

$$Q(f) = \pi\delta^2 \sum_{i=1}^{N_r \cdot N_\theta} w_i f(x_i, y_j) = \pi\delta^2 \sum_{i=1}^{N_r} \sum_{j=1}^{N_\theta} \tilde{w}_i f(r_i \cos(\theta_j), r_i \sin(\theta_j)), \quad (3.4)$$

where N_r is the number of radial points, N_θ is the number of equally spaced angles, and w_i and \tilde{w}_i are weights in $[0, 1]$ interval. The weights and cubature points are calculate by a modification of the Elhay-Kautsky Legendre quadrature method [5, 11]. The modified method uses an implicit QL algorithm to diagonalize the symmetric tridiagonal Jacobi matrix [15].

3.1.2 Nonuniform cubature

Alternatively, we can transform the disk into a square, and then use a two dimensional Guassian quadrature to approximate the integral. First, we transform the disk with radius δ to the rectangle $[0, \delta] \times [0, 2\pi]$ in the $r - \theta$ plane. Next, we transform this rectangle to a $[0, 1] \times [0, 1]$ square on the $\xi - \eta$ plane by using a linear transformation

$$r = \delta\xi, \quad \theta = 2\pi\eta,$$

that has the Jacobian $2\pi\delta$. Using these transformations, the original integral

$$\int_0^\delta \int_0^{2\pi} f(r \cos(\theta), r \sin(\theta)) r d\theta dr$$

now has the form

$$\int_0^1 \int_0^1 f(\delta\xi \cos(2\pi\eta), \delta\xi \sin(2\pi\eta)) \delta\xi 2\pi\delta \, d\eta \, d\xi.$$

For the integration over the interior of a general disk, we use generalised Gaussian quadrature rules described in [14]. This yields the following approximation for the integral, in which N is the number of weights w_i , and ξ_i and η_i are the positions corresponding to the i th point in the 1D Gaussian quadrature:

$$Q(f) = \sum_{i=1}^N \sum_{j=1}^N w_i w_j 2\pi \delta^2 \xi_i f(\delta\xi_i \cos(2\pi\eta_j), \delta\xi_i \sin(2\pi\eta_j)) = \sum_{m=1}^{N^2} \tilde{w}_m f(x_m, y_m). \quad (3.5)$$

Here $x_m = \delta\xi_i \cos(2\pi\eta_j)$, $y_m = \delta\xi_i \sin(2\pi\eta_j)$ and $\tilde{w}_m = w_i w_j 2\pi \delta^2 \xi_i$.

The distribution of the points for both uniform and nonuniform cubature formulas can be seen in Figure 3.1. Experimental results reveal that the uniform cubature (3.4) performs better in cases the interpolated function $f(x, y)$ is a bivariate polynomial, whereas the nonuniform cubature (3.5) when $f(x, y)$ is an arbitrary nonlinear function [10].

A natural question is which cubature rule performs better for the system (3.2). One way to determine the convergence of the cubature formulas is to apply (3.4) and (3.5) to the function $g_1(r) g_2(\theta) I_0 r$, where

$$I_0(r, \theta) = \frac{100}{2\pi s^2} \exp\left(-\frac{r^2}{2s^2}\right). \quad (3.6)$$

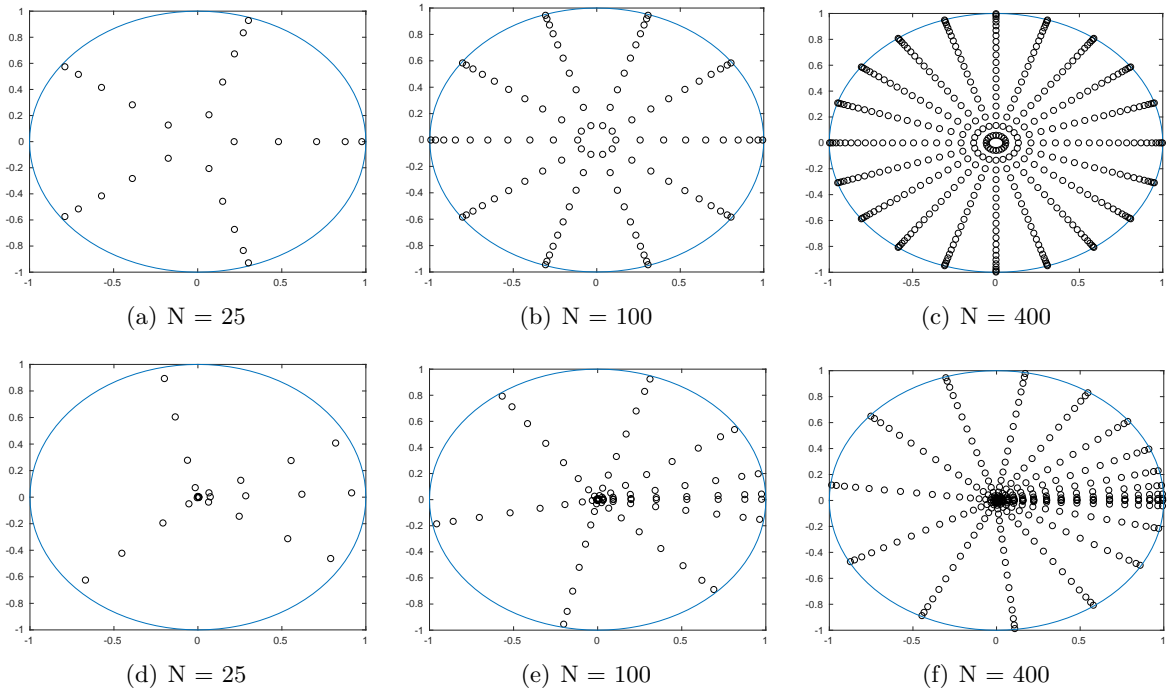


Figure 3.1: The distribution of points (N) using cubature rules for the integration over the unit disk. *Top panel*: uniform Cubature rules, *bottom panel*: nonuniform Cubature rules.

is a Gaussian distribution with deviation s and centered at zero. This resembles the initial conditions for I at the origin, as we will see later in Section 5. The exact solution of the integral over a disk of radius δ is given by

$$\int_0^\delta \int_0^{2\pi} g_1(r) g_2(\theta) I_0 r d\theta dr = 5000 \left(2\delta - \sqrt{2\pi} s \operatorname{Erf} \left[\frac{\delta}{\sqrt{2}s} \right] \right).$$

Figure 3.2 shows the convergence of the two cubature rules over the disk of radius δ as δ goes to zero. We observe that the nonuniform cubature (3.5) gives much smaller errors (close to machine precision) when more than 100 points are used, compared to cubature (3.4). The uniform cubature (3.4) is third-order accurate, similarly (3.5) is third order for $n = 25$ and 100 points.

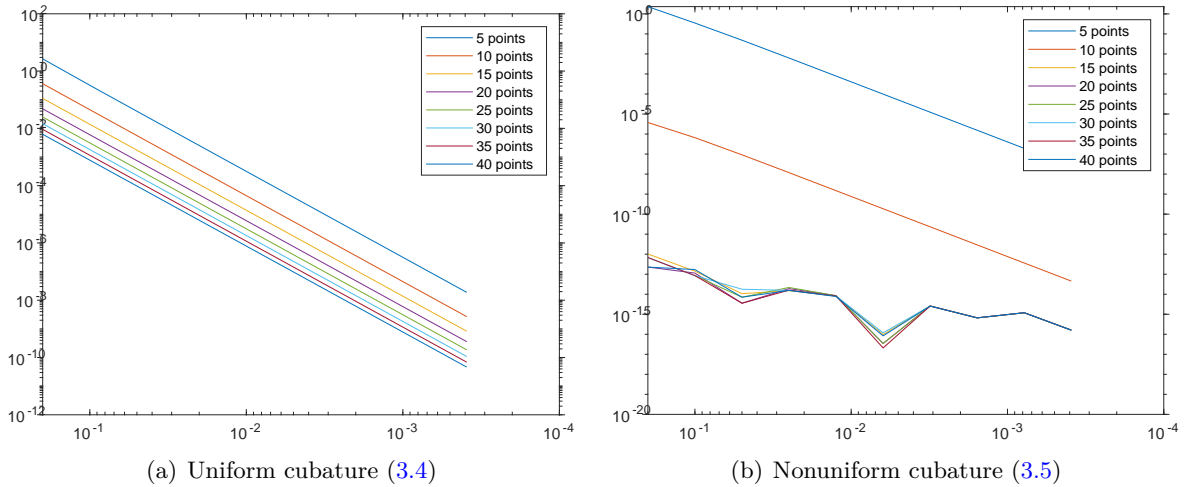


Figure 3.2: The errors using different number of cubature points. For practical reasons, the square roots of the numbers of the points are written next to the figure.

The performance of the cubature formulas depends on the choice of interpolation and who the interpolation is carried out. For the system (1.5) one can choose to interpolate only the function $I(t, \bar{x}, \bar{y})$ (and thus derive the system (3.2)) or interpolate all together the integrated function $G(x, y, r, \theta) I(t, \bar{x}, \bar{y})$. As mentioned before, bilinear interpolation can be used since it preserves the positivity of the function. One possibility is to use higher order interpolations, like cubic or spline, but in these cases the preservation of the required properties cannot be guaranteed. However, numerical experiments show that both cubic and spline interpolation result in a positive interpolant for sufficiently small spatial step sizes. A better choice is the use of a structure-preserving interpolation instead of cubic interpolation. This can be accomplished by a monotone interpolation that uses cubic Hermite splines [4, 8].

In the case of the interpolating only the function $I(t, \bar{x}, \bar{y})$, we get similar results for both cubature formulas. Using the same test function as before, we get the errors presented on Figure 3.3. As expected bilinear interpolation gives larger errors and spline interpolation performs much better.

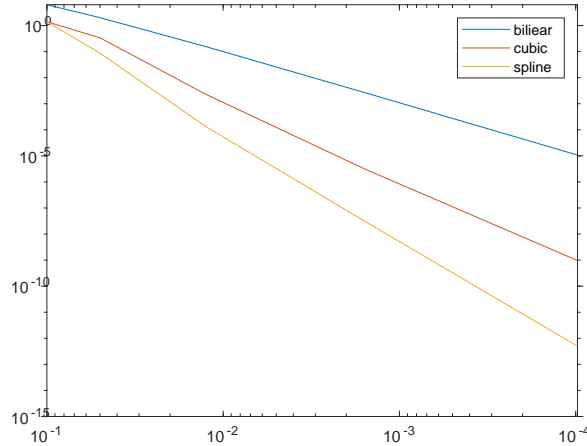


Figure 3.3: The errors using different interpolation methods.

4 Time integration methods

The next step is to use time integration methods to solve the system of ordinary differential equations (3.2). First we study sufficient and necessary time step restrictions such that the forward Euler method satisfies properties $D_1 - D_4$, and then discuss how high order SSP Runge-Kutta methods can be applied to (3.2).

4.1 Explicit Euler scheme and qualitative properties

Let us apply the explicit Euler method to the system (3.2) on the $[0, t_f]$ interval, and choose the time step to be $\tau > 0$, i.e. $\mathcal{N}\tau = t_f$ where \mathcal{N} is the number of steps in the method. After the full discretization we get the set of algebraic equations

$$\begin{cases} S^{n+1} = S^n - \tau S^n \circ T^n - c\tau S^n, \\ I^{n+1} = I^n + \tau S^n \circ T^n - b\tau I^n, \\ R^{n+1} = R^n + b\tau I^n + c\tau S^n, \end{cases} \quad (4.1)$$

in which S^n, I^n, R^n denotes the numerical solutions at $n\tau$, i.e. the previously described $\{S_{k,l}\}$, $\{I_{k,l}\}$, $\{R_{k,l}\}$ and $\{T_{k,l}\}$ matrices after the n th iteration of the method. Also, \circ is the element-by-element or Hadamard product of these matrices.

Now we examine the choices of timestep τ such that the method (4.1) gives solutions which behave well qualitatively and satisfy conditions $D_1 - D_4$.

Theorem 4.1. *Property D_2 holds without restrictions, and if the time step satisfies*

$$\tau \leq \min \left\{ \frac{1}{c + \tilde{w} \kappa^2 N M}, \frac{1}{b} \right\}, \quad (4.2)$$

where

$$M = \max_{(x_k, y_l) \in \mathcal{G}} \{S(0, x_k, y_l) + I(0, x_k, y_l) + R(0, x_k, y_l)\},$$

$$\kappa = \max\left\{\max_{r \in (0, \delta)} \{g_1(r)\}, \max_{\theta \in [0, 2\pi]} \{g_2(\theta)\}\right\},$$

$\tilde{w} = \max_{i,j} (w_{i,j})$, and N is the number of the points in $\mathcal{Q}(x, y)$, then properties D_1 , D_3 and D_4 also hold.

Proof. The proof is similar to the one of Theorem 2 in [19]. We prove the statement by induction for n , i.e., we first prove that the qualitative properties hold for the first step, and then we continue with the proof for an arbitrary step.

The nonnegativity of the values S^1 , I^1 and R^1 is true if $T^0 \geq 0$ and if (4.2) holds. By definition,

$$T_{k,l}^0 = \sum_{(x_{i,j}, y_{i,j}) \in \mathcal{Q}(x_k, y_l)} w_{i,j} g_1(r_i) g_2(\theta_j) \tilde{I}^0(x_k + r_i \cos(\theta_j), y_l + r_i \sin(\theta_j))$$

because we use the initial values to approximate the solution at time $t = 0$. Also, $\tilde{I}^0(x_k + r_i \cos(\theta_j), y_l + r_i \sin(\theta_j))$ might be an interpolated value, if the point in the cubature is not part of the spatial mesh. Because $\tilde{I}^0 \geq 0$, we get the nonnegativity of $T_{k,l}^0$, and consequently, our first step.

Now we suppose that the properties hold up to step n and we prove it for step $n + 1$. Property D_2 is trivial if we add up our equations. For D_3 , from the first equation of (4.1) we have

$$S_{k,l}^{n+1} = (1 - \tau(T_{k,l}^n + c))S_{k,l}^n,$$

from which we get the non-increasing property (because $T_{k,l}^n \geq 0$), and the nonnegativity if

$$\tau \leq \frac{1}{T_{k,l}^n + c} = \frac{1}{c + \sum_{(x_{i,j}, y_{i,j}) \in \mathcal{Q}(x_k, y_l)} w_{i,j} g_1(r_i) g_2(\theta_j) \tilde{I}^n(x_k + r_i \cos(\theta_j), y_l + r_i \sin(\theta_j))}. \quad (4.3)$$

(4.3) holds because of the left hand term on the right hand side of condition (4.2). The positivity of $I_{k,l}^n$ and $R_{k,l}^n$ can be shown similarly, since

$$I_{k,l}^{n+1} = (1 - b\tau)I_{k,l}^n + \tau S_{k,l}^n I_{k,l}^n,$$

and

$$R_{k,l}^{n+1} = R_{k,l}^n + b\tau I_{k,l}^n + c\tau S_{k,l}^n,$$

so these are also positive, and $R_{k,l}^n$ increases as n increases. \square

We can see from numerical experiments that the bound (4.2) is not strict, since larger choices for time step τ resulting in appropriate solutions, meaning that the method preserved the properties D_1 - D_4 . Because of this, we investigated two possible approaches which could result in a better bound.

(A1) We could use variable step sizes, namely

$$\tau_{n+1} = \min \left\{ \min_{k,l} \frac{1}{c + T_{k,l}^n}, \frac{1}{b} \right\}.$$

This way the timesteps are extremely strict, since if $\tau_{n+1} > \min_{k,l} \frac{1}{c + T_{k,l}^n}$, then one of the qualitative properties are violated. Thus, this method produces the best possible time steps, but would take more time to compute the values of $\min_{k,l} \frac{1}{c + T_{k,l}^n}$ at every step, and we cannot say anything about the time steps τ_n a priori. Moreover, as we can see in the Section 4.2, we can calculate such time steps at a given step only for one- and two-stages Runge–Kutta methods.

(A2) This approach investigates the connection between the condition $\tau_{n+1} = \min_{k,l} \frac{1}{c + T_{k,l}^n}$ and the bound (4.2). The main question is whether we can choose a less strict bound than (4.2) which would still guarantee that the condition $\tau \leq \frac{1}{c + T_{k,l}^n}$ holds for every k, l , and n . For this, we construct a matrix similar to $T_{k,l}^0$:

$$\tilde{T} := \mathcal{D}(M),$$

in which M is defined as before, and \mathcal{D} is the operator that constructs T^n from I^n in a way that $T^n = \mathcal{D}(I^n)$. This operator \mathcal{D} depends on the choice of the numerical integration and the points used in it, and also on $g_1(r)$ and $g_2(\theta)$. It is evident that if

$$\tau = \min \left\{ \frac{1}{c + \tilde{T}}, \frac{1}{b} \right\},$$

then the condition $\tau \leq \frac{1}{c + T_{k,l}^n}$ still holds, and $\frac{1}{c + \tilde{T}} \geq \frac{1}{c + \tilde{w} \kappa^2 NM}$, so this is a better bound. Numerical experiments show that this is also pretty close to the theoretically best bound which was calculated in approach (A1), so the relatively small increase of it may produce qualitatively bad solutions which violate one of the conditions D_1 – D_4 .

4.2 SSP Runge-Kutta methods

Forward Euler method is only first-order accurate, hence we would like to obtain step size restrictions for higher order Runge–Kutta methods. Note that the spatial discretizations discussed in Section 3 can be chosen so that errors from cubature formulas and interpolation are very small; therefore, it is substantial to have a high order method in time.

Consider a Runge–Kutta method in the Butcher form, and let K to be the coefficients' matrix given by

$$K = \begin{bmatrix} A & 0 \\ b^\top & 0 \end{bmatrix}.$$

If there exists $r > 0$ such that $(I + rK)$ is invertible, then the Runge–Kutta method can be expressed in the canonical Shu–Osher form

$$\begin{aligned} Q^{(i)} &= v_i Q^n + \sum_{j=1}^m \alpha_{ij} \left(Q^{(j)} + \frac{\tau}{r} F(Q^{(j)}) \right), \quad 1 \leq i \leq m+1 \\ Q^{n+1} &= Q^{(m+1)}, \end{aligned} \tag{4.4}$$

where the coefficient arrays α and v have non-negative components. The choice of parameter r gives rise to different Shu–Osher representations; thus we denote the Shu–Osher coefficients of (4.4) by α_r and v_r to emphasize the dependence on the parameter r . The Shu–Osher representation with the largest value of r such that $(I + rK)^{-1}$ exists and α_r, v_r have non-negative components is called optimal and attains the SSP coefficient

$$\mathcal{C} = \max\{r \geq 0 : \exists (I + rK)^{-1} \text{ and } \alpha_r \geq 0, v_r \geq 0\}.$$

We would like to investigate time step restrictions such that the numerical solution obtained by applying method (4.4) to the problem (3.2) satisfies properties $D_1 - D_4$. The following theorem provides the theoretical time step upper bound for these properties $D_1 - D_4$ are satisfied.

Theorem 4.2. *Consider the numerical solution obtained by applying a Runge–Kutta method (4.4) with SSP coefficient \mathcal{C} to the semi-discrete problem (3.2). Then property D_2 holds without any time step restrictions. Moreover, the properties D_1, D_3 and D_4 hold if the time step satisfies*

$$\tau \leq r \min \left\{ \frac{1}{c + \tilde{w} \kappa^2 N M}, \frac{1}{b} \right\}, \tag{4.5}$$

where

$$\begin{aligned} M &= \max_{(x_k, y_l) \in \mathcal{G}} \{S(0, x_k, y_l) + I(0, x_k, y_l) + R(0, x_k, y_l)\}, \\ \kappa &= \max \left\{ \max_{r \in (0, \delta)} \{g_1(r)\}, \max_{\theta \in [0, 2\pi]} \{g_2(\theta)\} \right\}, \end{aligned}$$

$\tilde{w} = \max_{i,j} (w_{i,j})$, and N is the number of the points in $\mathcal{Q}(x, y)$.

Proof. Firstly, in order to prove property D_2 it is convenient to consider the equivalent Butcher form

$$Q^{(i)} = Q^n + \tau \sum_{j=1}^m a_{ij} F(Q^{(j)}), \quad 1 \leq i \leq m \tag{4.6a}$$

$$Q^{n+1} = Q^n + \tau \sum_{i=1}^m b_i F(Q^{(i)}) \tag{4.6b}$$

of method (4.4), where the Butcher coefficient matrix

$$K = \begin{bmatrix} A & 0 \\ b^\top & 0 \end{bmatrix}$$

is related to the Shu–Osher coefficients by $K = \frac{1}{r}(I - \alpha_r)^{-1}\alpha_r$. Using (4.6b) we get

$$\begin{aligned} S^{n+1} &= S^n - \tau \sum_{j=1}^m S^{(j)}T^{(j)} - cS^{(j)}, \\ I^{n+1} &= I^n + \tau \sum_{j=1}^m S^{(i)}T^{(j)} - bI^{(j)}, \\ R^{n+1} &= R^n + \tau \sum_{j=1}^m bI^{(j)} + cS^{(j)}, \end{aligned}$$

and adding all the above equations yields

$$S^{n+1} + I^{n+1} + R^{n+1} = S^n + I^n + R^n, \quad \forall n.$$

The remainder of the proof deals with properties D_1 , D_3 and D_4 . We show that all quantities S, R, I remain positive, while S is non-increasing and R is increasing. At the i th stage we have

$$\begin{aligned} S^{(i)} &= v_i S^n + \sum_{j=1}^m \alpha_{ij} \left(S^{(j)} - \frac{\tau}{r} S^{(j)} T^{(j)} - \frac{\tau}{r} c S^{(j)} \right) \\ &= v_i S^n + \sum_{j=1}^m \alpha_{ij} S^{(j)} \left(1 - \frac{\tau}{r} T^{(j)} - \frac{\tau}{r} c \right). \end{aligned} \tag{4.7}$$

We claim that

$$0 \leq 1 - \frac{\tau}{r} T^{(j)} - \frac{\tau}{r} c \leq 1 \quad \text{for each } 1 \leq j \leq m. \tag{4.8}$$

Note that by definition $T_{k,l}^{(j)} \geq 0$ for every $1 \leq j \leq m$, and thus the second inequality in (4.8) holds independently of the value of τ . Moreover, $T_{k,l}^{(j)} \leq \tilde{w} \kappa^2 NM$ since $\tilde{I}^{(j)}$ is an interpolated value of $I^{(j)}$ and hence bounded by M . Choosing the step size such that

$$\tau \leq r \frac{1}{c + \tilde{w} \kappa^2 NM},$$

satisfies (4.8) and then (4.7) becomes

$$S^{(i)} \leq v_i S^n + \sum_{j=1}^m \alpha_{ij} S^{(j)}.$$

Consistency requires that $v_i + \sum_{j=1}^m \alpha_{ij} = 1$ for each $1 \leq i \leq m+1$ and hence

$$\begin{aligned} S^{(i)} &\leq \left(1 - \sum_{j=1}^m \alpha_{ij} \right) S^n + \sum_{j=1}^m \alpha_{ij} S^{(j)} \\ &\leq S^n - \sum_{j=1}^m \alpha_{ij} \left(S^n - S^{(j)} \right). \end{aligned} \tag{4.9}$$

Let $1 \leq q \leq m+1$ be the stage index such that $S^{(i)} \leq S^{(q)}$ for all $1 \leq i \leq m+1$. Then, taking $i = q$ in (4.9) yields

$$\begin{aligned} S^{(q)} &\leq v_i S^n + \sum_{j=1}^m \alpha_{qj} S^{(q)} \\ \left(1 - \sum_{j=1}^m \alpha_{qj}\right) S^{(q)} &\leq \left(1 - \sum_{j=1}^m \alpha_{qj}\right) S^n \\ S^{(q)} &\leq S^n. \end{aligned}$$

Therefore, $S^{(i)} \leq S^n$ for all $1 \leq i \leq m+1$. In particular for $i = m+1$ we have $S^{n+1} = S^{(m+1)} \leq S^n$. Also, S^{n+1} is non-negative since $S^{(i)} \geq 0$ for all $1 \leq i \leq m+1$.

For the population of the infected group I , we have at the i th stage that

$$\begin{aligned} I^{(i)} &= v_i I^n + \sum_{j=1}^m \alpha_{ij} \left(I^{(j)} + \frac{\tau}{r} (S^{(j)} T^{(j)} - b I^{(j)}) \right) \\ &= v_i I^n + \frac{\tau}{r} \sum_{j=1}^m \alpha_{ij} S^{(j)} T^{(j)} + \left(1 - \frac{\tau}{r} b\right) \sum_{j=1}^m \alpha_{ij} I^{(j)}. \end{aligned}$$

If $1 - \frac{\tau}{r} b \geq 0$, then $I^{(i)} \geq 0$; therefore, the time step bound $\tau \leq \frac{r}{b}$ must hold. Finally,

$$R^{(i)} = v_i R^n + \sum_{j=1}^m \alpha_{ij} \left(R^{(j)} + \frac{\tau}{r} b I^{(j)} + \frac{\tau}{r} c S^{(j)} \right) \geq R^n, \quad \forall i,$$

and hence, $R^{n+1} = R^{(m+1)} \geq R^n$.

Putting everything together, properties D_1 - D_4 are satisfied whenever

$$\tau \leq r \min \left\{ \frac{1}{c + \tilde{w} \kappa^2 N M}, \frac{1}{b} \right\}.$$

□

Remark 4.1. The bound 4.5 can be made less strict, and consequently better by the same argument described in approach (A2), by using the timestep

$$\tau = r \min \left\{ \frac{1}{c + \tilde{T}}, \frac{1}{b} \right\}, \quad (4.10)$$

in which \tilde{T} is the same as defined before. Note that approach (A1) cannot be used directly, since it would require the usage of different time steps at each stage of the method, affecting the overall accuracy. In practice the time-restriction (4.10) is only applicable to forward Euler and two-stage methods, because in such case \tilde{T} only relies on the previous solution.

5 Numerical experiments

In this section we confirm the results proved in the previous sections by using several numerical experiments. Computational tests are defined in a bounded domain and thus the choice of boundary conditions is important. Because we have no diffusion in our problem, we consider homogeneous Dirichlet conditions and we assume that there is no susceptible population outside of our domain. This means that we are going to assign a zero value to any point which lies outside of our rectangle in which the problem is defined. Using the aforementioned cubatures (3.4) and (3.5) in most cases the cubature points do not belong on the spatial grid. Special attention must be given to the corners and boundaries of the domain where cubature points assigned to gridpoints near the boundary lie outside of the domain. To be able to handle them, we are using ghost cells which are set to zero. This enables us to calculate the values corresponding to the cubature points lying outside of the domain.

For the numerical experiments we are choosing the following functions. Let $g_1(r)$ be a linearly decreasing function, which takes its maximum at $r = 0$ and becomes zero at $r = \delta$, i.e.,

$$g_1(r) := a(-r + \delta),$$

where a is a parameter as in (1.1). Also, we are going to use a non-constant $g_2(\theta)$ function, which is going to be symmetrical in a way that

$$g_2(\theta) := \beta \sin(\theta + \alpha) + \beta.$$

From now on, we are using the choices of $\alpha = 0$ and $\beta = 1$, assuming a northern wind on the domain. In our numerical experiments we are also using the choices $a = 100$, $b = 0.1$, $c = 0.01$, and $\delta = 0.05$.

Regarding the initial conditions, we assume that the number of susceptibles is constant on the whole domain, i.e., $S_{k,l}^0 = S_0 = 20$ for all k, l , and there are no recovered at the beginning, i.e. $R_{k,l}^0 = 0$ for all k, l . For the infected species, we use a Gaussian distribution concentrated at the middle of our domain $(A/2, B/2)$, and has standard deviation $s = \min(A, B)/10$:

$$I_{k,l}^0 = \frac{1}{2\pi s^2} \exp \left(-\frac{1}{2} \left[\left(\frac{h_1(k-1) - \frac{A}{2}}{s} \right)^2 + \left(\frac{h_2(l-1) - \frac{B}{2}}{s} \right)^2 \right] \right),$$

where $A = (K-1)h_1$ and $B = (L-1)h_2$ as mentioned in (3.6). We also set $A = B = 1$.

Our main aim in the next part is to observe whether our methods converge as expected. Since we cannot compute our exact solution, we are going to compute the errors using a reference solution, which will be computed by using the same parameters, but with a very small step size. The first task is to observe how well the different cubatures behave. As seen in Section 3, using more points in cubature (3.5) results in smaller errors, and also faster convergence. Numerical experiments show that it is indeed true for the system (3.2). The L_1 -norm errors can be seen in Figure 5.1. It is clear that for 25 or 100 points there is no remarkable difference between the interpolations, but for more cubature points cubic and spline interpolation perform better.

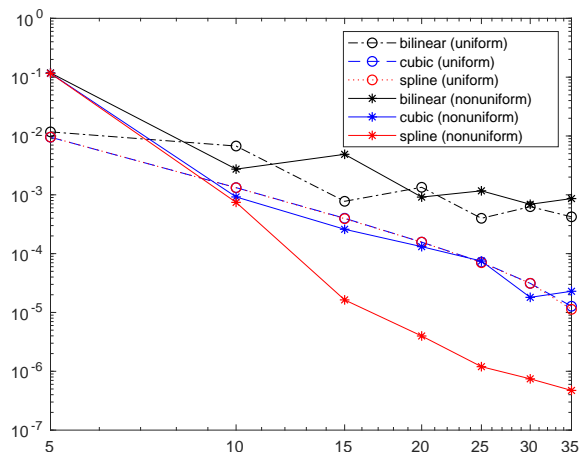


Figure 5.1: L_1 -norm errors using cubatures formulas (3.4) and (3.5) with n^2 points, $n \in \{5, 10, 15, 20, 25, 30, 35\}$ and different interpolations. The final time is chosen to be $t_f = 1$, the spacial step $h = 1/30$ and we used the ten-stage, fourth-order SSP Runge-Kutta method (SSPRK104).

τ	FE		IM		SSPRK22		SSPRK33		SSPRK104	
0.4290	9.9×10^{-3}		1.5×10^{-2}		2.6×10^{-4}		8.8×10^{-6}		1.8×10^{-8}	
0.2145	5.1×10^{-3}	0.96	7.6×10^{-3}	0.96	6.7×10^{-5}	1.94	1.2×10^{-6}	2.92	1.2×10^{-9}	3.93
0.1073	2.5×10^{-3}	1.05	3.8×10^{-3}	1.06	1.7×10^{-5}	1.95	1.6×10^{-7}	2.88	8.3×10^{-11}	3.87
0.0536	1.1×10^{-3}	1.20	1.6×10^{-3}	1.20	4.2×10^{-6}	2.06	2.0×10^{-8}	3.00	6.7×10^{-12}	3.96
0.0268	3.6×10^{-4}	1.57	5.5×10^{-4}	1.57	8.4×10^{-7}	2.30	2.2×10^{-9}	3.14	1.4×10^{-12}	3.17

Table 5.1: The errors and orders of using different time integration methods ("IM" denotes the method (2.19)), with final time $t_f = 1$, space steps $K = L = 20$, bilinear interpolation and the 10^2 point (Q1) cubature.

Bilinear interpolation results in similar errors for both cubatures (3.4) and (3.5). As it can be seen, cubic and spline interpolation perform the same for (3.4) and smaller errors are observed with spline interpolation and cubature (3.5).

Another important question is the order of the different time integration methods, i.e., is it beneficial to use the higher order ones rather than the first order Forward Euler, or the direct method described in Section 2.2. Numerical experiments show that the higher order schemes work as expected, namely that by using enough cubature points and grid points, a reasonably small error can be achieved.

Table 5.1 shows the convergence rates for various SSP Runge-Kutta method and the integral solution used in Section 2.2. We start with a reasonable timestep 0.429, which is below the bound described in approach (A2), and then successively dividing by 2. For the reference solution we use a time step that is the half of the smallest time step in our computations. It is evident that using higher order methods is better than solving the integral equation (2.17) numerically, and even the Forward Euler method produces smaller errors than scheme (2.19).

Finally, Figure 5.2 depict the numerical solution of the function S and I are plotted for different times. As we can see, the number of susceptibles decrease, and the number of infected moves towards the boundaries, while forming a wave. Both of them tend to the zero function, which confirms that the zero solution is indeed an asymptotically stable equilibrium, which was proved in Section 2.

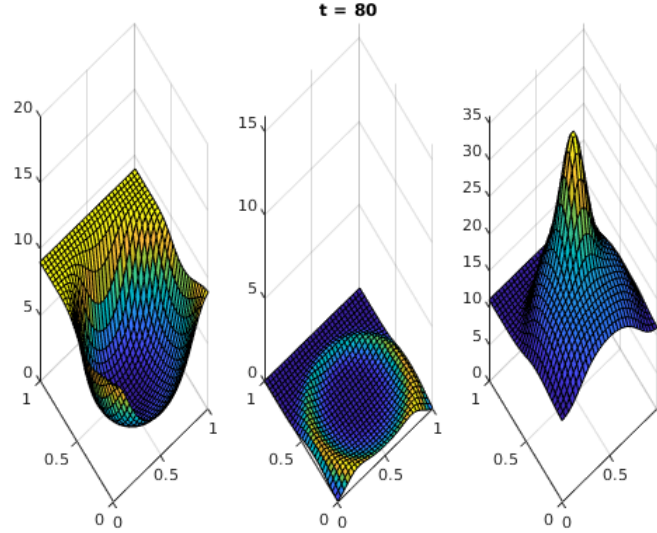


Figure 5.2: The number of susceptibles S (left), infected I (middle) and recovered R (right) at time $t_f = 80$. The SSPRK104 method has been used with nonuniform cubature (3.5) (225 cubature points) and spline interpolation. We used 30 grid points and $\delta = 0.05$.

6 Conclusions, further work

In this paper the SIR model for epidemic propagation is extended to include spatial dependence. The existence and uniqueness of the continuous solution were proved, along with properties corresponding to biological observations. For the numerical solution, different choices of cubature, interpolation and time integration methods are studied. It is shown that for a sufficient small time-step restriction, the numerical solution preserves a discrete analogue of the properties of the original continuous system. This bound was also refined, and an adaptive time step technique is also mentioned for the Explicit Euler method and for second-stage Runge–Kutta methods. These theorems were confirmed by numerical experiments, while the errors of cubature formulas and the order of accuracy of the time discretization methods are also discussed.

A possible extension of the work presented in this paper is to include diffusion in the system, and observe its effect on the system. Results for the preservation of qualitative properties can be potentially obtained. Moreover the include the births and natural deaths in the system and dropping the conservation property makes the model more realistic. It would be interesting to

study the influence of such modification in the behavior of the continuous and also the numerical solution.

Acknowledgement

The project has been supported by the European Union, co-financed by the European Social Fund (EFOP-3.6.3-VEKOP-16-2017-00002). The authors would like to thank Lajos Lóczi for his support.

References

- [1] Aronson, D. G., The asymptotic speed of propagation of a simple epidemic, *Nonlinear diffusion*, vol. 14, Pitman London, 1977, pp. 1–23.
- [2] Capasso, V. and Fortunato, D., [Stability results for semilinear evolution equations and their application to some reaction-diffusion problems](#), *SIAM Journal on Applied Mathematics*, 39 (1980), pp. 37–47.
- [3] Davis, P. J. and Rabinowitz, P., [Methods of numerical integration](#), Corrected reprint of the second (1984) edition, Dover Publications, Inc., Mineola, NY, 2007, pp. xii+612.
- [4] Dougherty, R. L., Edelman, A. S., and Hyman, J. M., [Nonnegativity-, monotonicity-, or convexity-preserving cubic and quintic Hermite interpolation](#), *Mathematics of Computation*, 52 (1989), pp. 471–494.
- [5] Elhay, S. and Kautsky, J., Algorithm 655: IQPACK: FORTRAN subroutines for the weights of interpolatory quadratures, *ACM Transactions on Mathematical Software (TOMS)*, 13 (1987), pp. 399–415.
- [6] Faragó, I. and Horváth, R., [On some qualitatively adequate discrete space-time models of epidemic propagation](#), *Journal of Computational and Applied Mathematics*, 293 (2016), pp. 45–54.
- [7] Faragó, I. and Horváth, R., [Qualitative properties of some discrete models of disease propagation](#), *Journal of Computational and Applied Mathematics*, 340 (2018), pp. 486–500.
- [8] Fritsch, F. N. and Carlson, R. E., [Monotone piecewise cubic interpolation](#), *SIAM Journal on Numerical Analysis*, 17 (1980), pp. 238–246.
- [9] Harko, T., Lobo, F. S. N., and Mak, M. K., [Exact analytical solutions of the susceptible-infected-recovered \(SIR\) epidemic model and of the SIR model with equal death and birth rates](#), *Applied Mathematics and Computation*, 236 (2014), pp. 184–194.
- [10] Jayan, S. and Kallur, N., Generalized Gaussian quadrature rules over an n-dimensional ball, *Pakistan Journal of Biotechnology*, 14 (Jan. 2017), pp. 423–428.
- [11] Kautsky, J. and Elhay, S., [Calculation of the weights of interpolatory quadratures](#), *Numerische Mathematik*, 40 (1982), pp. 407–422.

- [12] Kendall, D. G., Mathematical models of the spread of infection, *Mathematics and computer science in biology and medicine*, (1965), pp. 213–225.
- [13] Kermack, W. O. and McKendrick, A. G., [A contribution to the mathematical theory of epidemics](#), *Proceedings of the Royal Society of London. Series A*, 115 (1927), pp. 700–721.
- [14] Ma, J.-H., Rokhlin, V. V., and Wandzura, S. M., [Generalized Gaussian quadrature rules for systems of arbitrary functions](#), *SIAM Journal on Numerical Analysis*, 33 (1996), pp. 971–996.
- [15] Martin, R. S. and Wilkinson, J. H., [Handbook Series Linear Algebra: The implicit QL algorithm](#), *Numerische Mathematik*, 12 (1968), pp. 377–383.
- [16] Miller, J. C., [A note on the derivation of epidemic final sizes](#), *Bulletin of Mathematical Biology*, 74 (2012), pp. 2125–2141.
- [17] Miller, J. C., [Mathematical models of SIR disease spread with combined non-sexual and sexual transmission routes](#), *Infectious Disease Modelling*, 2 (2017), pp. 35–55.
- [18] Stroud, A. H., [Approximate calculation of multiple integrals](#), Prentice-Hall Series in Automatic Computation, Prentice-Hall, Inc., Englewood Cliffs, N.J., 1971, pp. xiii+431.
- [19] Takács, B., Horváth, R., and Faragó, I., Space dependent models for studying the spread of some diseases, *Computers & Mathematics with Applications*, (2019), (accepted).
- [20] Thieme, H. R., [A model for the spatial spread of an epidemic](#), *Journal of Mathematical Biology*, 4 (1977), pp. 337–351.